The Journal of Chemical Physics

Direct ΔMBPT(2) method for ionization potentials, electron affinities, and excitation energies using fractional occupation numbers

Cite as: J. Chem. Phys. **138**, 074101 (2013); https://doi.org/10.1063/1.4790626
Submitted: 15 November 2012 . Accepted: 24 January 2013 . Published Online: 15 February 2013

Ariana Beste, Álvaro Vázquez-Mayagoitia, and J. V. Ortiz

AIP Publishing

Direct ΔMBPT(2) method for ionization potentials, electron affinities, and excitation energies using fractional occupation numbers

Ariana Beste,[1,a)] Álvaro Vázquez-Mayagoitia,[2,b)] and J. V. Ortiz[3,c)]
[1]*Joint Institute for Computational Sciences, University of Tennessee, Oak Ridge, Tennessee 37831, USA*
[2]*Argonne Leadership Computing Facility, Argonne National Laboratory, Argonne, Illinois 60439, USA*
[3]*Department of Chemistry and Biochemistry, Auburn University, Auburn, Alabama 36849, USA*

(Received 15 November 2012; accepted 24 January 2013; published online 15 February 2013)

A direct method (D-ΔMBPT(2)) to calculate second-order ionization potentials (IPs), electron affinities (EAs), and excitation energies is developed. The ΔMBPT(2) method is defined as the correlated extension of the ΔHF method. Energy differences are obtained by integrating the energy derivative with respect to occupation numbers over the appropriate parameter range. This is made possible by writing the second-order energy as a function of the occupation numbers. Relaxation effects are fully included at the SCF level. This is in contrast to linear response theory, which makes the D-ΔMBPT(2) applicable not only to single excited but also higher excited states. We show the relationship of the D-ΔMBPT(2) method for IPs and EAs to a second-order approximation of the effective Fock-space coupled-cluster Hamiltonian and a second-order electron propagator method. We also discuss the connection between the D-ΔMBPT(2) method for excitation energies and the CIS-MP2 method. Finally, as a proof of principle, we apply our method to calculate ionization potentials and excitation energies of some small molecules. For IPs, the ΔMBPT(2) results compare well to the second-order solution of the Dyson equation. For excitation energies, the deviation from equation of motion coupled cluster singles and doubles increases when correlation becomes more important. When using the numerical integration technique, we encounter difficulties that prevented us from reaching the ΔMBPT(2) values. Most importantly, relaxation beyond the Hartree-Fock level is significant and needs to be included in future research. © *2013 American Institute of Physics*. [http://dx.doi.org/10.1063/1.4790626]

I. INTRODUCTION

Modern quantum chemistry is a high precision tool to calculate molecular properties, explain experimental data, and predict reaction pathways. The underlying physics, however, is extremely complicated and in almost all applications, approximations are employed. In chemistry, we are generally interested in energy differences (reaction energies and barriers, spectroscopic data, solvation energies, etc.). To not exacerbate intrinsic errors of the theoretical method, initial and final states need to be described consistently and with errors lower than the quantity of interest. Conceptually, the simplest approach to calculate energy differences is to apply the same method to both states, which proves successful to explore the potential energy surface and to obtain reaction energies and barriers.

The focus of this work is the computation of energy differences between ground and electronic excited states, where the number of electrons may change. In such cases, the definition of the final state becomes more challenging. Within the self-consistent field (SCF) approach, the initial and final states can be characterized through the occupation of the orbitals. To avoid variational collapse in the excited state, the orbital occupation has to be fixed by symmetry or by constraint. Taking the energy difference between the variationally optimized final and initial states yields the ΔSCF method, applicable to Hartree-Fock or density functional theory (DFT).

One of the disadvantages of the ΔSCF method is that the energy difference is typically much smaller than the total energies of the initial and final states (possibly orders of magnitude depending on system size and quantity of interest). The resulting precision problem is avoided in direct difference methods, where energy differences are computed directly without explicit determination of initial and final states. A simple example of a direct method at the Hartree-Fock level is the use of Koopmans's theorem to calculate ionization potentials (IPs) and electron affinities (EAs).[1] At the correlated level, IPs, EAs, and excitation energies can be computed directly with the equation-of-motion coupled cluster (EOM-CC)[2,3] or Fock space coupled cluster[4,5] methods. Related approaches to obtain IPs and EAs at various levels of correlation[6,7] are based on the electron propagator.[8] Excitation energies can be derived from the polarization propagator,[8] which leads in its uncorrelated form to the random phase approximation (RPA) or, equivalently, to time-dependent Hartree-Fock theory.[9] RPA is closely linked to time-dependent density functional theory,[10] where correlation is approximated through the exchange-correlation potential. A simplification of the RPA is the configuration interaction singles (CIS) method, where the excited state is a linear combination of singly excited Hartree-Fock

[a)]Electronic mail: bestea@ornl.gov.
[b)]Electronic mail: alvaro@anl.gov.
[c)]Electronic mail: ortiz@auburn.edu.

determinants. If dynamic correlation of the ground and excited state is expressed up to second order, the resulting method is CIS-MP2,[11] which is similar in spirit to the D-ΔMBPT(2) (direct ΔMBPT(2)) method for excitation energies described in this paper.

The direct methods mentioned above have in common that initial and final states are not described at the same level of theory. Typically, orbitals of the ground state are utilized to express the property of interest using an expansion (linear or exponential) or through an iterative solution of the Dyson equation. A distinct advantage of Δ methods is that initial and final states are treated equally and, consequently, there is no need for the relaxation of orbitals. In the here developed D-ΔMBPT(2), we aim to keep that benefit but to avoid the aforementioned precision problem. Energies of the initial and final states are given as a perturbation expansion up to second order of a variationally optimized Hartree-Fock wave function with appropriate occupation numbers. The energy difference between final and initial state is obtained through numerical integration of the energy derivative with respect to a chosen parameter.

The numerical integration technique has been previously applied to calculate IPs, EAs, and excitation energies at the ΔSCF level.[12] The general idea is the same as the one underlying the thermodynamic integration technique in molecular dynamics,[13,14] the adiabatic connection in the context of DFT,[15] or the integral Hellmann-Feynman theorem.[16] A coupling parameter is introduced, which defines a pathway that connects two different states of a system. At the extreme points of complete coupling or no coupling the system has to correspond to a physically meaningful state. Along the path, however, the parameter can be chosen by convenience. Let λ be such a parameter. At $\lambda = 0$ the system is in its initial state and at $\lambda = 1$ the system is in its final state. The energy difference between initial and final state ΔE is then given by

$$\Delta E = E(1) - E(0) = \int_0^1 \frac{\partial E}{\partial \lambda} d\lambda. \tag{1}$$

Instead of potentially large energies, the energy derivative with respect to λ is evaluated, which is on the same order of magnitude as the energy difference itself and can lead to an efficient computational scheme. Essential for the success of such approach is that the energy derivative be smooth within the parameter range.

If Eq. (1) is employed to calculate IPs, an obvious choice for parameter λ is the occupation number of the ionized orbital. The integration path between end points is then characterized by fractional occupation numbers, which do not have to be physically meaningful but the corresponding orbitals may provide a superior reference in post Hartree-Fock methods.[17] In the context of the X_α formalism, a midpoint integration scheme results in Slater's transition state concept,[18] which is shown in Ref. 19. Slater's concept is based on a perturbation expansion of the initial and final state about a common occupation number and has been successfully applied to the calculation of IPs[20] and to rationalize the operator choice within an effective one-particle theory yielding improved IPs as a measure for functional accuracy within density functional theory.[21] Related to Slater's approach, transition energies and probabilities can be obtained by minimizing the energy of a transition operator,[22,23] which has been utilized within the context of electron propagator theory[24] to compute valence and core IPs.

In the following, we will apply the concept represented by Eq. (1) to obtain second-order IPs, EAs, and excitation energies and compare the resulting equations to various techniques. Test calculations for ionization potentials and excitation energies are given for small molecules.

II. THEORY AND IMPLEMENTATION

In Ref. 12, the feasibility of a numerical integration scheme to calculate IPs, EAs, and excitation energies has been tested for uncorrelated wavefunctions. To include correlation at the lowest level (extension to higher order is possible), an energy expression up to second order in perturbation

$$E^{(2)} = E^{HF} + \frac{1}{4} \sum_{ijab} \frac{\langle ij \| ab \rangle \langle ab \| ij \rangle}{\epsilon_i + \epsilon_j - \epsilon_a - \epsilon_b} \tag{2}$$

can be inserted into Eq. (1). E^{HF} is the Hartree-Fock energy and ϵ_m is the orbital energy of orbital m; antisymmetric two-electron integrals are used. $i, j, k, \ldots$ refer to orbitals occupied in the reference determinant, $a, b, c, \ldots$ refer to virtual orbitals, and we will use $m, n, p, \ldots$ for general orbitals. The Hamiltonian used to derive Eq. (2) is partitioned into the zeroth-order Hamiltonian, which is chosen to be the diagonal one-electron Fock operator, and the perturbation, given as the two-electron contribution to the exact Hamiltonian subtracted by the Coulomb and exchange parts of the Fock operator. The Hartree-Fock energy is recovered as the sum of zeroth- and first-order energies.

The correlated ground, ionized, and excited state, as well as the state containing an additional electron are characterized by an occupation number or a set of occupation numbers in the Hartree-Fock reference function, which is selected as the parameter λ in Eq. (1). The derivative of the Hartree-Fock energy with respect to an occupation number has been discussed in Ref. 12. In order to obtain the derivative of the correlation energy, we write the correlation energy in terms of occupation numbers. The second-order expression in $V = \frac{1}{4} \sum_{mnpq} \langle mn \| pq \rangle m^\dagger n^\dagger qp$ as a function of occupation numbers has been derived by evaluating the connected contributions to the free energy,[25] where the zeroth-order Hamiltonian is a non-interacting Hamiltonian including kinetic energy and nuclear-electronic interaction. Since we use a slightly different partitioning of the Hamiltonian (as described in the previous paragraph), the second-order expression is given by

$$E_c^{(2)} = \frac{1}{4} \sum_{mnpq}^{all} n_m n_n (1 - n_p)(1 - n_q) \frac{\langle mn \| pq \rangle^2}{\epsilon_m + \epsilon_n - \epsilon_p - \epsilon_q}, \tag{3}$$

where the remaining term in Ref. 25 cancels with Coulomb and exchange contributions from the Fock operator. n_m is the occupation number of orbital m. Note, that the distinction between occupied and unoccupied orbitals does not exist when fractional occupation is allowed. At zero K the expression

reduces to the integer-occupation second-order expression. The partial derivative of $E_c^{(2)}$ with respect to an occupation number is obtained as

$$\frac{\partial E_c^{(2)}}{\partial n_r} = \frac{1}{2}\sum_{mpq}^{all} n_m(1-n_p)(1-n_q)\frac{\langle mr\|pq\rangle^2}{\epsilon_m+\epsilon_r-\epsilon_p-\epsilon_q} - \frac{1}{2}\sum_{mnq}^{all} n_m n_n(1-n_q)\frac{\langle mn\|rq\rangle^2}{\epsilon_m+\epsilon_n-\epsilon_r-\epsilon_q} + \text{higher-order terms.} \quad (4)$$

When differentiating with respect to n_r in Eq. (4), r is a general orbital index. The first term in Eq. (4) corresponds to differentiation, where r is a hole index in the corresponding energy expression with integer occupancy; whereas the second term corresponds to differentiation, where r is a particle index. The higher-order terms are a consequence of the dependence of the orbital energies on the occupation number[26]

$$\epsilon_s = h_{ss} + \sum_n^{all} n_n\langle ns\|ns\rangle. \quad (5)$$

The partial derivative of the orbital energy with respect to an occupation number is given by

$$\frac{\partial \epsilon_s}{\partial n_r} = \langle rs\|rs\rangle. \quad (6)$$

Using Eq. (6), we obtain the higher-order terms as

$$HOT = -\frac{1}{4}\sum_{mnpq}^{all} n_n n_m(1-n_p)(1-n_q) \times \frac{\langle mn\|pq\rangle^2}{(\epsilon_m+\epsilon_n-\epsilon_p-\epsilon_q)^2} \times \left(\langle rm\|rm\rangle + \langle rn\|rn\rangle - \langle rp\|rp\rangle - \langle rq\|rq\rangle\right). \quad (7)$$

In Eqs. (4) and (7) the implicit choice of orbitals is the set that makes the second-order energy at any given occupation stationary with respect to orbital change. Here, we use orbitals for which the SCF energy is stationary with respect to orbital change. As a consequence, we may neglect orbital relaxation effects beyond what is captured at the SCF level; i.e., the term $\frac{\partial E^{HF}}{\partial \phi_r}\frac{\partial \phi_r}{\partial n_r} = 0$ but $\frac{\partial E_c^2}{\partial \phi_r}\frac{\partial \phi_r}{\partial n_r} \neq 0$.

The IP is defined as the energy difference between the ionized and the neutral system; i.e., $E(0) = E^N$ and $E(1) = E^{N-1}$ in Eq. (1), where N is the number of electrons in the system. If ionization occurs from a single orbital i, while the remaining orbitals keep integer occupation, the second-order IP is obtained by setting $\lambda = 1 - n_i$ and expressing the energy through second order

$$E^{(N-1)} - E^N = IP_i = \int_0^1 \frac{\partial E^{(2)}}{\partial \lambda} d\lambda = \int_0^1 \frac{\partial E^{(2)}}{\partial n_i}\frac{\partial n_i}{\partial \lambda} d\lambda, \quad (8a)$$

$$= \int_0^1 \left(-\epsilon_i - \frac{\partial E_c^{(2)}}{\partial n_i}\right) d\lambda, \quad (8b)$$

$$= \int_1^0 \left(\epsilon_i + \frac{\partial E_c^{(2)}}{\partial n_i}\right) dn_i. \quad (8c)$$

$\frac{\partial E_c^{(2)}}{\partial n_i}$ is derived from Eq. (4) by setting all orbital occupations to integer values, except for orbital i, which can play the role of an occupied or an unoccupied orbital. The sums are split into terms independent of orbital i and terms that include orbital i. The partial derivative is then given by

$$\frac{\partial E_c^{(2)}}{\partial n_i} = \frac{1}{2}\sum_{j}^{occ}\sum_{ab\neq i}^{virt}\frac{\langle ij\|ab\rangle^2}{\epsilon_i+\epsilon_j-\epsilon_a-\epsilon_b} \quad (I)$$

$$+ \sum_{j}^{occ}\sum_{a}^{virt}(1-n_i)\frac{\langle ij\|ia\rangle^2}{\epsilon_j-\epsilon_a} \quad (I)$$

$$- \frac{1}{2}\sum_{kj\neq i}^{occ}\sum_{a}^{virt}\frac{\langle kj\|ia\rangle^2}{\epsilon_k+\epsilon_j-\epsilon_i-\epsilon_a} \quad (II)$$

$$- \sum_{j}^{occ}\sum_{a}^{virt} n_i\frac{\langle ij\|ia\rangle^2}{\epsilon_j-\epsilon_a} \quad (II)$$

$$+ \text{higher-order terms.} \quad (9)$$

Terms I and II correspond to the diagonal diagrammatic integer-occupation expressions given in Figure 1. Notice, the diagrams represent complete sums (for instance, the first and second terms are realized by diagram I). We use antisymmetrized Goldstone diagrams,[27] where unlabeled lines are summed over. The interpretation of the diagrams follows conventional rules[27] except that due to fractional occupation of orbital i, the sums over occupied and virtual orbitals include orbital i. The denominators are most easily derived from the generating energy diagrams. By convention, the

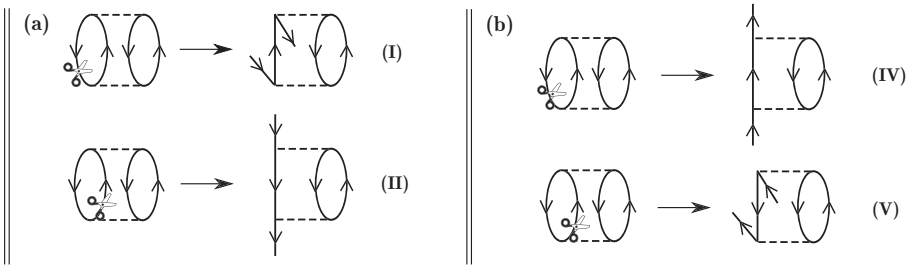

FIG. 1. (a) Diagonal diagrammatic expressions corresponding to terms I and II in Eq. (9), (b) diagonal diagrammatic expressions corresponding to terms IV and V in Eq. (12); diagrams on the left of the arrows correspond to second-order energy terms, where the scissors indicate which line is cut to obtain the diagrams on the right of the arrows.

resolvent lines are omitted with the understanding that an energy denominator is included between each successive pair of vertices.

Notice that differentiation with respect to the occupation number in the second-order energy expression corresponds to a systematic opening of the second-order energy diagrams, indicated by scissors in Figure 1. If a particle line is cut, the line direction in the IP term is changed, since the open line has to have hole character to describe an ionization. This is a reflection of the fact that a partially occupied orbital contributes as a hole as well as a particle in the correlation expression, as discussed above.

The higher-order terms in Eq. (9) resulting from the dependence of the orbital energies on the occupation numbers are derived from Eq. (7) and given by

$$\begin{aligned} HOT_{IP} = &-\frac{1}{4}\sum_{jk\neq i}^{occ}\sum_{ab\neq i}^{virt}\frac{\langle kj\|ab\rangle^2}{(\epsilon_k+\epsilon_j-\epsilon_a-\epsilon_b)^2} \\ &\times(\langle ik\|ik\rangle+\langle ij\|ij\rangle-\langle ia\|ia\rangle-\langle ib\|ib\rangle) \\ &-\frac{1}{2}\sum_{j}^{occ}\sum_{ab\neq i}^{virt}n_i\frac{\langle ij\|ab\rangle^2}{(\epsilon_i+\epsilon_j-\epsilon_a-\epsilon_b)^2} \\ &\times(\langle ij\|ij\rangle-\langle ia\|ia\rangle-\langle ib\|ib\rangle) \\ &-\frac{1}{2}\sum_{jk\neq i}^{occ}\sum_{b}^{virt}(1-n_i)\frac{\langle kj\|ib\rangle^2}{(\epsilon_k+\epsilon_j-\epsilon_i-\epsilon_b)^2} \\ &\times(\langle ik\|ik\rangle+\langle ij\|ij\rangle-\langle ib\|ib\rangle) \\ &-2\sum_{j}^{occ}\sum_{b}^{virt}n_i(1-n_i)\frac{\langle ij\|ib\rangle^2}{(\epsilon_j-\epsilon_b)^2} \\ &\times(\langle ij\|ij\rangle-\langle ib\|ib\rangle)\,. \end{aligned} \tag{10}$$

We separated terms according to the dependence on orbital i. Equation (10) is represented by diagram III in Figure 2. The unconventional bracket used in Figure 2 signifies that only the subset of terms in which the line indices that are connected by the bracket are the same, are representative of term III. Interestingly, these diagrams can be derived from a subset of third-order energy diagrams by cutting the bubble as indicated by the scissors in Figure 2. The full set of third-order energy diagrams can be found in Ref. 27.

The EA is defined as the energy difference between the neutral system and the system with an additional electron; i.e., $E(0) = E^{N+1}$ and $E(1) = E^N$ in Eq. (1). Analogous to the IP, if attachment occurs into a single orbital a, while the remaining orbitals keep integer occupation, the second-order EA is obtained by setting $\lambda = n_a$ and expressing the energy through second order

$$E^N - E^{(N+1)} = EA_a = \int_0^1 \frac{\partial E^{(2)}}{\partial\lambda}d\lambda = \int_0^1 \frac{\partial E^{(2)}}{\partial n_a}\frac{\partial n_a}{\partial\lambda}d\lambda, \tag{11a}$$

$$= \int_0^1 \left(\epsilon_a + \frac{\partial E_c^{(2)}}{\partial n_a}\right) dn_a. \tag{11b}$$

As in the IP case, the Hartree-Fock contribution to the EA is the orbital energy, which is augmented by a correlation term. The integrand in Eqs. (8) and (11) can, therefore, be regarded as a correlated orbital energy.

$\frac{\partial E_c^{(2)}}{\partial n_a}$ is derived from Eq. (4) by setting all orbital occupation to integer value, except for orbital a. The sums are split according to the participation of orbital a. We obtain

$$\begin{aligned} \frac{\partial E_c^{(2)}}{\partial n_a} = &\frac{1}{2}\sum_{i}^{occ}\sum_{bc\neq a}^{virt}\frac{\langle ai\|bc\rangle^2}{\epsilon_i+\epsilon_a-\epsilon_b-\epsilon_c} && (IV) \\ &+\sum_{i}^{occ}\sum_{b}^{virt}(1-n_a)\frac{\langle ai\|ab\rangle^2}{\epsilon_i-\epsilon_b} && (IV) \\ &-\frac{1}{2}\sum_{ij\neq a}^{occ}\sum_{b}^{virt}\frac{\langle ij\|ab\rangle^2}{\epsilon_i+\epsilon_j-\epsilon_a-\epsilon_b} && (V) \\ &-\sum_{i}^{occ}\sum_{b}^{virt}n_a\frac{\langle ai\|ab\rangle^2}{\epsilon_i-\epsilon_b} && (V) \\ &+\text{ higher-order terms.} \end{aligned} \tag{12}$$

The diagrammatic expressions of terms IV and V are given in Figure 1. Note that the sums over occupied and virtual orbitals include orbital a. Equivalent to the IP diagrams, the EA diagrams can be derived by cutting the lines of the second-order energy diagrams. If a hole line is cut, the direction of the line changes, representing the ambiguous character of an orbital with fractional occupation number.

The higher-order terms in Eq. (12) derived from Eq. (7) are given by

$$\begin{aligned} HOT_{EA} = &-\frac{1}{4}\sum_{ij\neq a}^{occ}\sum_{bc\neq a}^{virt}\frac{\langle ji\|bc\rangle^2}{(\epsilon_j+\epsilon_i-\epsilon_b-\epsilon_c)^2} \\ &\times(\langle aj\|aj\rangle+\langle ai\|ai\rangle-\langle ab\|ab\rangle-\langle ac\|ac\rangle) \end{aligned}$$

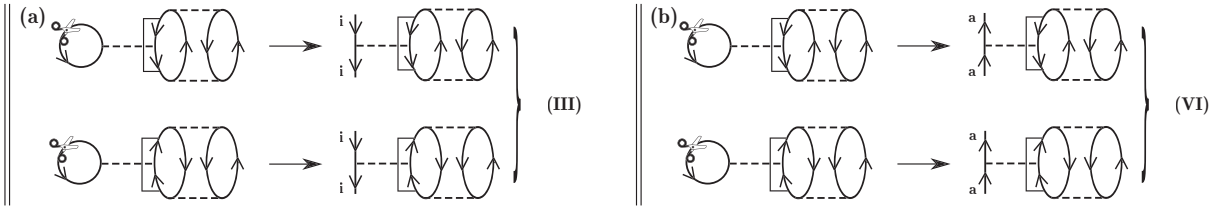

FIG. 2. (a) Diagonal diagrammatic expressions corresponding to term III in Eq. (10), (b) diagonal diagrammatic expressions corresponding to term VI in Eq. (13); the unconventional bracket indicates that the line indexes are the same; diagrams on the left of the arrows correspond to third-order energy terms, where the scissors show which line is cut to obtain the diagrams on the right of the arrows.

$$
\begin{aligned}
&- \frac{1}{2} \sum_{i}^{occ} \sum_{bc \neq a}^{virt} n_a \frac{\langle ai \| bc \rangle^2}{(\epsilon_a + \epsilon_i - \epsilon_b - \epsilon_c)^2} \\
&\times (\langle ai \| ai \rangle - \langle ab \| ab \rangle - \langle ac \| ac \rangle) \\
&- \frac{1}{2} \sum_{ij \neq a}^{occ} \sum_{b}^{virt} (1 - n_a) \frac{\langle ji \| ba \rangle^2}{(\epsilon_j + \epsilon_i - \epsilon_b - \epsilon_a)^2} \\
&\times (\langle aj \| aj \rangle + \langle ai \| ai \rangle - \langle ab \| ab \rangle) \\
&- 2 \sum_{i}^{occ} \sum_{b}^{virt} n_a (1 - n_a) \frac{\langle ai \| ba \rangle^2}{(\epsilon_i - \epsilon_b)^2} \\
&\times (\langle ai \| ai \rangle - \langle ab \| ab \rangle) \qquad (13)
\end{aligned}
$$

The diagrammatic expressions of terms VI representing Eq. (13) and the corresponding third-order energy diagrams can be found in Figure 2.

For an excitation between orbital ϕ_i and ϕ_a, the system change is characterized by the occupation numbers n_i and n_a,

$$dE = \frac{\partial E}{\partial n_a} dn_a + \frac{\partial E}{\partial n_i} dn_i. \qquad (14)$$

Since the occupation of orbital a increases by the same amount as the occupation of orbital i decreases, only a single parameter λ is needed. Expressing the energy through second order with $n_i = 1 - \lambda$ and $n_a = \lambda$, Eq. (1) becomes

$$
\begin{aligned}
\Delta E_{i \to a} &= \int_0^1 \left(\frac{\partial E^{(2)}}{\partial n_a} \frac{\partial n_a}{\partial \lambda} + \frac{\partial E^{(2)}}{\partial n_i} \frac{\partial n_i}{\partial \lambda} \right) d\lambda, \\
&= \int_0^1 \left(\epsilon_a - \epsilon_i + \frac{\partial E_c^{(2)}}{\partial n_a} - \frac{\partial E_c^{(2)}}{\partial n_i} \right) d\lambda, \qquad (15)
\end{aligned}
$$

where $\Delta E_{i \to a}$ is the energy difference between the excited and ground state. The partial derivatives $\frac{\partial E_c^{(2)}}{\partial n_i}$ and $\frac{\partial E_c^{(2)}}{\partial n_a}$ are given in the Appendix. In Eqs. (9) and (12) only one orbital was allowed to be fractionally occupied, whereas orbitals i and a have fractional occupation numbers in Eq. (15). The partial derivatives of the energy with respect to the occupation number of orbital i (Eq. (9)) and a (Eq. (12)) can be expressed as the derivative with respect to a general orbital r. We chose to write a separate equation for the IPs and EAs to make the connection to the diagrammatic expressions in Fig. 1. In the Appendix, we give the derivatives in Eq. (15) with respect to the occupation number of a general orbital r, where the occupation of orbital s is also fractional but all other orbitals have integer occupation. Notice, that the leading terms do not depend on how many orbitals are fractionally occupied, only the number of terms with explicit dependence on the occupation numbers of the partially occupied orbitals increases. Since the terms with explicit dependence on the occupation numbers only occur because we restrict the sums of the leading terms to not include fractionally occupied orbitals, the diagrammatic expressions of the derivatives of the correlation energy in Eq. (15) are the sum of the diagrammatic expressions for the IP of orbital i and the EA of orbital a (Figures 1 and 2).

When optimized Hartree-Fock orbitals at fractional occupation are used in the correlated expressions, orbital relaxation in response to ionization, electron attachment, and excitation is introduced through integration over the parameter. The integrands are the Hartree-Fock contributions, i.e., the orbital energies, and a second-order correlation term. Notice, however, that the Hartree-Fock contributions are not Koopmans's values but are the fully relaxed ΔSCF results for ionization and electron attachment if the integration is carried out exactly.[12] We have previously shown that the orbital energy difference in Eq. (15) yields the ΔSCF result for excitation.[12] Since correlation effects are expressed using a fixed reference determinant at variable occupation, relaxation is treated at the SCF level only.

III. DISCUSSION AND COMPARISON WITH OTHER METHODS

The derivative of the second-order energy with respect to occupation numbers has been considered in the context of DFT[28] to analyze the behavior of the energy as a function of partial charges. The exact energy as a function of fractional charges is a straight line between the integer points,[29] which is violated by common density functionals. Higher-order terms were neglected in Ref. 28 and only variations in frontier orbitals were considered. Since we would like to describe valence and core-ionization and attachment processes in different orbitals leading to various excitations, we are interested in the energy derivative with respect to the occupation of a general orbital.

The second-order, integer-occupation expression for IPs (Eq. (9)) can alternatively be derived by taking the energy difference of the $N - 1$- and N-particle system, where the energies are expressed up to second order in a common set of orbitals. In the $N - 1$-particle system the sum over occupied orbitals is reduced by terms where an occupied orbital is equal to i and the sum over virtual orbitals includes terms where a virtual orbital is equal to i. The result is the second-order IP given as the sum of the negative orbital energy ϵ_i and the negative of the second-order terms of Eq. (9). (The sign change is due to the integration variable change in Eq. (8).) This consistency is reassuring, given that our goal was to express this same energy difference in Eq. (8). For EAs, the second-order, integer-occupation expression of Eq. (12) can be derived by taking the energy difference of the N-particle system and the $N + 1$ particle system. The corresponding expression for $\Delta E_{i \to a}^{c}$ can be obtained by taking the difference of the second-order energy of the excited and ground state expressed in a common set of orbitals. In the excited system, the sum over occupied orbitals is reduced by terms where j, k, or l is equal to i, the sum over unoccupied orbitals is decreased by terms where b or c is equal to a. The sum over virtual orbitals includes terms where b or c is equal to i and the sum over occupied orbitals is augmented by terms where j, k, or l is equal to a.

Further, the IP and EA diagrams in Figure 1 can be deduced from an effective Fock-space coupled-cluster Hamiltonian,[4,5] which was used to formulate an exact one-particle theory, yielding exact IPs and EAs.[30] The second-order approximation of the occupied-occupied and the virtual-virtual block of the effective Hamiltonian leads to the corresponding second-order IPs and EAs.[31] In Eq. (3), we

used canonical Hartree-Fock orbitals implying that the off-diagonal Fock elements are zero. We then recognize that diagrams I and II in Figure 1 are the diagonal terms of the remaining non-zero second-order diagrams of the occupied-occupied block (diagrams VI and VII in Fig. 4 in Ref. 31). Equivalently, diagrams IV and V in Figure 1 are the diagonal terms of the remaining non-zero second-order diagrams of the virtual-virtual block in Ref. 31.

Notice, that through differentiation one only obtains diagonal terms, whereas the effective Hamiltonian derived from Fock-space coupled-cluster is diagonalized to yield IPs and EAs. Diagonalization can be interpreted as a relaxation of the orbitals, which is incorporated in the method presented herein through Eq. (1). In fact, diagonalization of the effective Hamiltonian causes severe limitations due to the intruder state problem and renders the effective Hamiltonian approach impractical.[31] The intruder state problem is largely avoided when the energy dependence in the correlation potential is retained and the corresponding equations are solved for a single IP or EA at a time, which is the case in the partitioned equation of motion approach,[2,3] in propagator theory,[8] and in the method described here. For a small reference space, intruder states may not present a complication. In that case, the advantage of an energy independent effective Hamiltonian or linear response methods is, of course, that all states of interest are obtained in a single calculation.

The close relationship between the effective Hamiltonian obtained from Fock-space coupled-cluster, equation of motion coupled-cluster and propagator theory has been shown previously.[30] Using electron propagator theory, the lowest-order correction to Koopmans's theorem IPs can be obtained as the first iteration of the second-order diagonal self-energy,[8] which again leads to diagrams I and II of Figure 1. The third-order diagrams of Figure 2 can be identified as the diagonal terms of the constant-energy contribution to the third-order self-energy,[32–34] where the restrictions indicated by the brackets are lifted. We note, that the self-energy of the second-order IP has been analyzed in terms of correlation and relaxation contributions by splitting the sum represented by diagram II in Fig. 1 into sums where i is included and where it is not (same as in this work but with integer occupation).[35] The second integer-occupation expression of term II in Eq. (9) is the lowest-order relaxation correction to Koopmans's value and may facilitate a more efficient numerical integration over occupation numbers. In Ref. 24, fractional occupation numbers have been exploited and the first iteration of the resulting equations coincides with the four terms of Eq. (9).

Finally, we seek a connection between the D-ΔMBPT(2) method for excitation energies and second-order methods based on configuration interaction singles or Tamm-Dancoff approximation. In CIS, the excited state is expressed as a linear combination of excited Slater determinants obtained by promoting one electron from an occupied orbital in the Hartree-Fock wave function into a virtual orbital. Diagonalization of the Hamiltonian in the space of singly excited determinants yields excitation energies. Due to Brillouin's theorem, the inclusion of single excitations amounts to an orbital rotation, which provides orbital relaxation. The CIS wave function can, therefore, be thought of as a Hartree-Fock quality wave function for the excited state. Treatment of dynamical second-order correlation effects in the CIS excited state and the ground state leads to the CIS-MP2 method.[11] The excited and ground state are also expressed through second order in the D-ΔMBPT(2) method but instead of supplying orbital relaxation through diagonalization in the space of single-excited determinants, relaxation effects are included through the use of fractional occupation numbers and subsequent integration. A direct comparison between the two methods is difficult because the second-order expansion of the CIS wave function includes triple excitations and single excitations from the CIS wave function, whereas these terms do not occur in the D-ΔMBPT(2) method due to the use of a relaxed excited state wave function. An advantage of the D-ΔMBPT(2) method is that the unperturbed ground and excited states are treated equally, whereas they are not in the CIS-MP2 method. Also, the excitation energy correction in CIS-MP2 is defined as an energy difference between total MP2 energies; our intent here is the derivation of a direct scheme. An improvement over the CIS-MP2 is the CIS(D),[36] where scaling is reduced from $\mathcal{O}(N^6)$ to $\mathcal{O}(N^5)$ and where size intensivity[37] is restored. Size intensivity[37] had been violated in the equation for the triple excitations of the CIS-MP2 method, where disconnected terms appear. We would like to point out that all diagrams listed here are connected, which guarantees size extensivity[27] for any value of fractional occupation. Further developments include the SCS-CIS(D)[38] and the SOS-CIS(D)[39] approaches and the corresponding SCS-CC2 and SOS-CC2 methods,[40,41] where empirical parameters (spin scaling) are introduced. The SOS methods can be implemented as $\mathcal{O}(N^4)$ algorithms. In the D-ΔMBPT(2) method, the most expensive step in the calculation of the IPs, EAs, and excitation energies including the higher-order terms is the transformation of the two-electron integrals into the MO basis, which scales as $\mathcal{O}(N^5)$. To reduce this cost, established methods, such as the resolution of the identity,[42] or approximations based on a reduced basis set[43] can be applied.

IV. APPLICATIONS

We calculated IPs and excitation energies for a small number of molecules: H_2O, CH_2O, NH_3, CH_4, and N_2. Geometries were obtained with the MBPT(2) method and a cc-pvtz basis set. Equation (9) and the corresponding equations given in the Appendix are evaluated using optimized Hartree-Fock orbitals at fractional occupation. We used a locally modified version of the NWChem program package.[44] IPs and excitation energies are computed by solving the integral in Eqs. (8) and (15) utilizing a Legendre-Gauss quadrature. The Legendre-Gauss interpolation is defined on an interval between −1 and 1. Instead of changing the interval limits, we choose to use half of the interpolated integral (between 0 to 1) because the energy derivative does not have a symmetry element at 0. Equation of motion coupled cluster singles and doubles (EOM-CCSD) results for excitation energies are computed with the NWChem program package using a cc-pvtz plus Dunning-Hay double Rydberg basis set,[45] ionization potential EOM-CCSD values for valence IPs are calculated with GAMESS[47] utilizing an uncontracted cc-pvtz basis

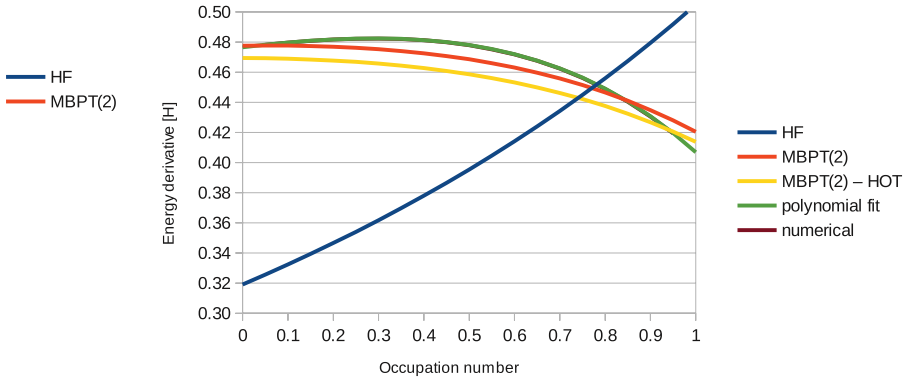

FIG. 3. Energy derivative as a function of the occupation number of the partially occupied HOMO corresponding to the HOMO IP of H_2O. Data points were recorded in intervals of 0.1 electrons.

set. Singlet excitation is achieved by exciting an electron from α-spin orbital i into α-spin orbital a, triplet excitation is accomplished by exciting an electron from α-spin orbital i into β-spin orbital a.

Typical atomic orbital basis sets are contracted in the core region. Since we calculate core as well as valence IPs, an uncontracted basis set is expected to be superior. For the calculation of excitation energies we anticipate that the inclusion of Rydberg functions is important. We tested a cc-pvtz, a completely uncontracted cc-pvtz, and a cc-pvtz plus Dunning-Hay double Rydberg basis set[45] for IPs, EAs, and excitation energies of H_2O, see the supplementary material.[46] The ionization potentials are not very sensitive to the basis set and vary within less than 0.1 eV except for the core IP, where the IP using an uncontracted cc-pvtz basis set is 0.5 eV higher than the IP calculated with the cc-pvtz basis set. For the EAs and excitation energies, the contracted basis set is sufficient. However, the inclusion of Rydberg functions has a large effect on EAs and excitation energies. Because water with an additional electron has no bound state, the Hartree-Fock EAs are determined by the quality of the basis set and approach zero for a large enough basis set.[48] The effect of Rydberg functions on excitation energies depends on the excitation type; i.e., the lowest B2 excitation energy is reduced by 0.4 eV, whereas the lowest A1 excitation energy is reduced by 12.1 eV. For the remaining calculations we used a completely uncontracted cc-pvtz basis set for the computation of IPs and a cc-pvtz plus Dunning-Hay double Rydberg basis set[45] for excitation energies.

Figure 3 shows the energy derivative as a function of the occupation number of the partially occupied HOMO corresponding to the HOMO IP (integrand in Eq. (8b)) and Figure 4 depicts the energy derivative as a function of the occupation number of the partially occupied HOMO corresponding to the HOMO-LUMO excitation (integrand in Eq. (15)) in H_2O. The graphs were obtained by recording data points in intervals of 0.1 electrons. For the HOMO IP, there is a striking difference between the Hartree-Fock derivative $(-\epsilon_i)$ and the correlated derivative, for which the slope is opposite. The correlation effect is not as strongly pronounced for the HOMO-LUMO excitation. For comparison, we included the MBPT(2) derivative without the higher-order terms and observe that the higher-order terms cause a shift of the derivative to higher values but, as expected, contribute significantly less than the second-order terms. In order to assess the magnitude of the orbital relaxation term beyond what is captured at the Hartree-Fock level, we plotted the derivative of a 5th-order polynomial obtained as a fit to the MBPT(2) total energies. Hidden by the polynomial fit is the numerical energy derivative using an interval of 0.1 electrons. The overlap of

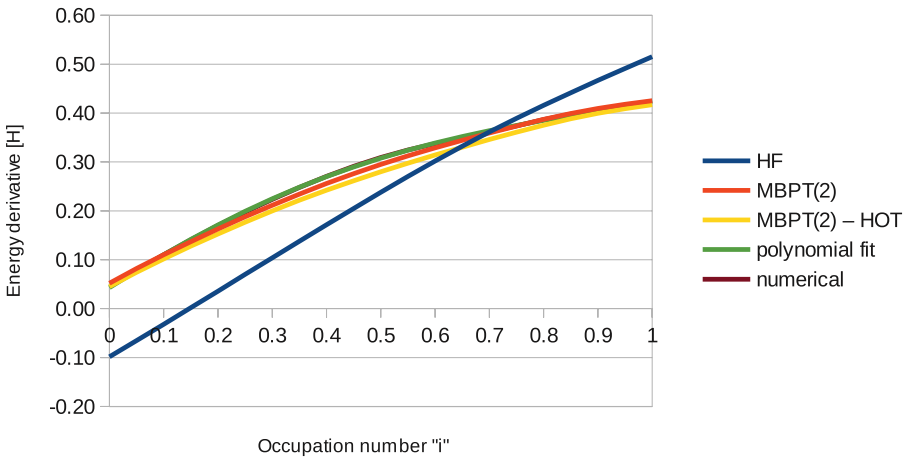

FIG. 4. Energy derivative as a function of the occupation number of the partially occupied HOMO corresponding to the HOMO-LUMO excitation in H_2O. Data points were recorded in intervals of 0.1 electrons.

numerical derivative and polynomial fit gives us confidence that the polynomial fit is representative. Indeed, the ΔMBPT(2) value of 12.69 eV for the HOMO IP is reproduced from the fit using 4 Legendre-Gauss quadrature points. The difference between the polynomial fit and the MBPT(2) derivative is the remaining relaxation term, which is on the order of the higher-order contribution stemming from the dependence of the orbital energies on the occupation number. The supplementary material[46] includes the energy derivatives as a function of occupation for all five IPs and the first three excitation energies of H_2O. For the IPs, the total Hartree-Fock and MBPT(2) energies as a function of the orbital occupation are included as well. The total energies appear to be linear; i.e., the curvature difference apparent in the derivatives cannot be recognized by visual inspection. For the interested reader, the graphs of the energy derivatives corresponding to the excitation energies are augmented by graphs showing the individual contributions from electron donating and electron receiving orbitals in the supplementary material.[46]

We analyzed the convergence behavior of the IPs and the first three excitation energies of H_2O with respect to the number of Legendre-Gauss quadrature points. The corresponding data can be found in the supplementary material.[46] For the valence IPs, the D-ΔMBPT(2) value is converged using only two quadrature points, for the core IP six quadrature points are necessary. The corresponding D-ΔHF values (numerical integration of $-\epsilon_i$) converge slower. Since for the excitation energies the energy derivative is taken with respect to the occupation number of two orbitals simultaneously, we observe slower convergence; i.e., within 8-10 quadrature points. We chose to use six quadrature points for the reported D-ΔMBPT(2) values in Table I (IPs) and eight quadrature points for the reported D-ΔMBPT(2) and D-ΔHF values in Table II (excitation energies).

Table I contains the IPs for H_2O, CH_2O, CH_4, NH_3, and N_2 obtained with the ΔHF, ΔMBPT(2), and the D-ΔMBPT(2) methods. These values are compared to Koopmans's values, experimental results, IP-EOM-CCSD values, and TOEP2 results.[24] The latter is a second-order approximation to the electron propagator using the transition operator method. Remembering that the solution of the propagator requires the iteration of the Dyson equation, this can be viewed as a second-order benchmark method. Comparing Koopmans's values with the ΔHF and ΔMBPT(2) results, we confirm that error cancellation occurs for Koopmans's values of valence IPs:[1] relaxation effects decrease Koopmans's IPs while correlation effects increase the valence IPs. Error cancellation is less effective for core IPs because relaxation tends to be dominant and the ΔHF method often provides a reasonable approximation (N_2 is an exception). The importance of relaxation effects for core IPs has motivated a recent variational coupled-cluster based approach, where ΔSCF values are reproduced through the application of the single excitation operator using an exponential ansatz.[49] For IPs in the range

TABLE I. Ionization potentials in eV; a completely uncontracted cc-pvtz basis set is used, geometries are calculated with MBPT(2)/cc-pvtz.

	Sym.	Koopmans	ΔHF	ΔMBPT(2)	D-ΔMBPT(2)	TOEP2[24]	EOM-CCSD	Exp.[a]
H_2O	A_1	559.34	538.90	539.96	541.32	539.48		539.86
	A_1	36.61	34.01	33.83	33.77[b] (35.61)			
	B_1	19.23	17.32	18.99	18.93	18.68	18.76	18.51
	A_1	15.77	13.21	14.94	14.83	14.56	14.69	14.74
	B_2	13.74	10.91	12.69	12.58	12.29	12.41	12.78
CH_2O	A_1	559.85	537.91	539.67	540.37	538.5		539.48
	A_1	308.58	293.81	295.50	295.83[b] (296.30)			294.47
	A_1	38.12	34.78	34.31	34.22[b] (59.05)			
	A_1	23.69	22.25	22.24	21.58			
	B_2	18.84	17.66	17.29	17.28		17.41	16.6
	A_1	17.67	14.52	16.44	16.14		16.03	16.0
	B_1	14.50	12.28	14.78	14.56		14.52	14.5
	B_2	12.04	9.40	11.26	10.79	10.38	10.77	10.88
CH_4	A_1	304.89	290.55	290.74	292.87	291.15		290.86
	A_1	25.70	24.20	23.93	24.12			
	T_2	14.85	13.50	14.44	14.55	14.34	14.40	13.6, 14.40 (15.0)
NH_3	A_1	422.69	405.05	405.84	407.50[b] (405.58)			405.6
	A_1	31.00	28.92	28.66	28.79			
	E	16.96	15.23	16.60	16.67		16.46	15.8 (16.5)
	A_1	11.65	9.38	10.90	10.96	10.65	10.73	10.85
N_2	A_{1g}	426.86	419.37	404.86	407.40	409.63		409.9
	A_{2u}	426.77	419.26	404.77	407.59			409.9
	A_{1g}	39.69	37.15	35.64	35.81			
	A_{2u}	21.30	20.16	18.26	18.74	18.59	18.93	18.78
	E_u	16.48	15.06	17.23	17.70	17.38	17.05	16.98
	A_{1g}	17.17	15.58	15.27	15.73	15.47	15.55	15.60

[a]Reference from which experimental ionization potentials were obtained: core,[50] valence.[51]

[b]Analytical continuation is used, values in parentheses are quadrature results.

TABLE II. Vertical excitation energies in eV; the cc-pvtz plus Dunning-Hay double Rydberg[45] basis set is used, geometries are calculated with MBPT(2)/cc-pvtz.

	Sym.	ΔHF	D-ΔHF	ΔMBPT(2)	D-ΔMBPT(2)	EOM-CCSD	Exp.[a]
H_2O	^{1}B2	6.19	6.21	7.65	7.54	7.58	7.4
	^{1}A2	7.95	7.97	9.56	9.60	9.36	9.1
	^{1}A1	8.64	8.66	10.17	10.23	9.89	9.7
CH_2O	^{1}A2	2.58	...	4.19	...	4.03	4.07
	^{1}B2	6.00	6.02	7.66	7.27	7.22	7.11
	^{1}B2	6.89	6.90	8.56	8.27	8.10	7.97
	^{1}A1	6.89	6.86	8.64	8.38	8.17	8.14
CH_4	^{1}T2	9.79	9.80	10.59	10.82	10.66	
	^{3}T2	9.67	9.68	10.40	10.72	10.34[b]	10.9
	^{1}A1	10.99	10.97	11.89	12.09	11.88	
NH_3	^{1}A1	5.40	5.42	6.60	6.67	6.61	5.7
	^{1}E	6.82	6.84	8.23	8.34	8.14	7.3
	^{1}A1	7.27	6.96	8.54	8.33	8.60	7.9
N_2	$^3\Pi_g$	7.53	7.68[c]	8.06	8.11[c]	8.16[d]	8.04
	$^1\Pi_g$	8.34	8.44[c]	8.89	8.84[c]	9.55[d]	9.31
	$^1\Sigma_u^-$	10.47	10.58[c]	9.37	9.95[c]	10.23[d]	9.92

[a]References from which experimental excitation energies were obtained: H_2O,[52] CH_2O,[52] CH_4,[48] NH_3,[53] N_2.[54]
[b]Instead of EOM-CCSD value, the CCSD energy difference between ground state singlet and triplet is given.
[c]Analytic continuation is used.
[d]Value from Ref. 55.

of 20–35 eV, correlation decreases the ΔHF IPs to a small extent. Despite the general trend of error cancellation for Koopmans's valence IPs, the valence IPs for N_2 are predicted to be in the wrong order using Koopmans's approximation. Orbital relaxation effects (ΔHF values) do not correct the IP order but the inclusion of second-order correlation (and higher) allows for an accurate description of the ionization spectrum of N_2. We observe that the performance of the ΔMBPT(2) method is similar to the TOEP2 method when compared to experiment. We also notice that the valence IPs computed with the ΔMBPT(2) methods for H_2O, CH_4, NH_3, and N_2 deviate from the IP-EOM-CCSD results by less than 0.3 eV with the exception of the lowest A_{2u} ionization in N_2. The difference to IP-EOM-CCSD values is larger for CH_2O, indicating that correlation effects are increasingly important.

However, when the derivative of the energy with respect to the occupation number is integrated to yield IPs, the deviation from the ΔMBPT(2) values can be a few tenths of an eV and tends to be larger for core IPs. This implies that orbital relaxation effects beyond what is captured at the SCF level are important, particularly where relaxation is dominant. (See, for instance, left panel of Figure 1 of the supplementary material,[46] which shows the MBPT(2) derivative with and without higher-order terms and the energy derivative obtained from a polynomial fit of the total energies for the core IP of H_2O; the difference between the MBPT(2) derivative and the polynomial fit is indicative of the second-order orbital relaxation effects.) For some IPs in Table I we used analytical continuation. This means that we used the energy derivative in only part of the interval between 0 and 1 to fit to a 5th order polynomial. We then took the derivative of the polynomial to perform the integration that yielded the IPs. The energy derivatives and energies as a function of occupation number for the second highest A1 IP in H_2O, the second and third highest A1 IP in CH_2O, and the highest A1 IP in NH_3 are given in the supplementary material.[46] At certain values of n_i the MBPT(2) derivative behaves erratically, while the Hartree-Fock derivative $(-\epsilon_i)$ remains smooth. This can be explained by looking at the third term of Eqs. (9) and (10). If two (generally positive) orbital energies of unoccupied orbitals are subtracted from two (generally negative) orbital energies of occupied orbitals, the denominator has a nonzero value. However, if orbital i takes the role of an unoccupied orbital, its (generally negative) orbital energy is subtracted and the denominator can become very small or even tend to zero. For instance, for CH_2O, we observe that the denominator in term three of Eqs. (9) and (10) becomes zero at $n_i = 0.85$ and $i = 3$, $k = 6$, $j = 7$, and $b = 13$. The energy difference between orbitals k and i increases as a function of n_i whereas the energy difference between orbitals b and j decreases. At $n_i = 0.85$ the two energy differences are the same. The effect is larger for higher-order terms because the sum of orbital energies in the denominator is squared. Note, the total energy can also show irregularities (see Eq. (3) and the energy as a function of occupation for the third highest A1 IP of CH_2O in the supplementary material[46]). Similar trends can occur for excitation energies, see, for instance, the individual contributions to the A1 excitation in H_2O displayed in the supplementary material.[46]

Table II shows the lowest vertical excitation energies from the HOMO for H_2O, CH_2O, CH_4, and NH_3. For N_2 excitations from the HOMO and an excitation from the second highest occupied orbital ($^1\Sigma_u^-$) are included. Again, the ΔHF results represent excitation energies where orbital relaxation is accounted for (at the HF level). When correlation is added to obtain the ΔMBPT(2) results, the excitation energy increases (with the exception of the $^1\Sigma_u^-$ excitation in N_2). For H_2O, CH_2O, CH_4, and N_2 the largest deviation

of the ΔMBPT(2) from the experimental value is 0.59 eV (second lowest ^{1}B2 of CH_2O). For NH_3, the deviation increases to up to 0.93 eV. However, the calculation of vertical excitation energies does not account for structural rearrangement in response to the electronic excitation. For NH_3 the structural relaxation is large since the symmetry changes from C_{3v} in the ground state to D_{3h} in the excited state. A better bench mark for the ΔMBPT(2) results are vertical excitation energies calculated with the EOM-CCSD method (included in Table II), where correlation effects from single and double excitation are accounted for to infinite order. For H_2O, CH_4, NH_3, and N_2 the difference between the ΔMBPT(2) and the EOM-CCSD values does not exceed 0.3 eV. Again, the N_2 $^1\Sigma_u^-$ excitation, which involves a π_u to π_g transition, is an exception, where the difference is larger (0.86 eV). Notice that compared to the experiment both methods have rather large deviations (0.31 eV EOM-CCSD and 0.55 eV ΔMBPT(2)). For CH_2O, where correlation effects are also expected to be important to describe the π-system, differences to the EOM-CCSD values up to 0.48 eV are detected.

We observe again, that the difference between the D-ΔMBPT(2) and the ΔMBPT(2) method is non-negligible. This is predominantly caused by residual orbital relaxation not accounted for at the Hartree-Fock level. In addition, potential inaccuracies are introduced due to the nature of the Hartree-Fock potential,[48] which generally predicts positive energies for unoccupied orbitals. This has been discussed previously[12] and a piece-wise integration or a path quadratic in λ has been suggested. Comparison of the D-ΔHF to the ΔHF values in Table II shows that this error is small. An exception is the second lowest ^{1}A1 excitation in NH_3. This, however, reveals a different problem. The supplementary material[46] contains the energy derivative and its contributions as a function of the HOMO occupation number for the second lowest ^{1}A1 excitation in NH_3. At 0.72 electrons a discontinuity occurs in the orbital energy, which affects the second-order curves as well. The discontinuity is caused by a sudden change of the electronic state and introduces errors in the numerical integration procedure (D-ΔHF as well as D-ΔMBPT(2)). Further, Table II does not show a D-ΔHF or D-ΔMBPT(2) value for the lowest excitation in CH_2O. Here, we also encounter a sudden change of the electronic state; the supplementary material[46] includes the energy derivative and the energy as a function of HOMO occupation for the HOMO-LUMO excitation in CH_2O. At 0 occupation ϵ_i is positive (typically ϵ_i is negative in the entire integration interval). As soon as orbital i is partially occupied, the orbital energy becomes negative since orbital i is now variationally determined. Since the electronic state at the interval end point differs from the electronic state in the remainder of the interval, the numerical integration scheme cannot be applied. We also encountered difficulties for N_2, where we were unable to converge to the correct Hartree-Fock energy for some fractional occupation numbers. We used analytical continuation as explained above. We notice that relaxation effects beyond the Hartree-Fock level are particularly large for the N_2 $^1\Sigma_u^-$ state, which may be rationalized by the fact that the excitation involves the second highest occupied molecular orbital, whereas all other excitations occur from the HOMO.

V. CONCLUSIONS

We have introduced a direct method to obtain second-order IPs, EAs, and excitation energies, which we termed D-ΔMBPT(2). The ΔMBPT(2) is defined as the second-order extension of the ΔHF method. Instead of calculating energy differences of total energies, energy derivatives with respect to occupation numbers are evaluated, which can be regarded as correlated orbital energies in the IP and EA case and a correlated orbital energy difference in the excitation case. In contrast to linear-response methods, relaxation is fully included at the SCF level up to numerical precision through the integration of the energy derivatives over the appropriate occupation range. Initial and final states are treated at the same level of approximation. This is important when finite basis sets are used, where the basis set is potentially better suited to describe the ground than the ionized, attached, or excited state if ground and excited states are not treated equally. The D-ΔMBPT(2) method can be extended to higher-order perturbation by taking energy derivatives of higher-order energy expressions with respect to occupation numbers and integrating over the appropriate parameter range.

The method described here is, in contrast to DFT methods, self-interaction free and applicable to charge-transfer excitations. Since the D-ΔMBPT(2) is not limited to linear-response problems, double or higher excitations energies can be evaluated by specifying the appropriate excitation in the SCF excited wave function. However, similar to CIS based methods, if higher excitations mix with predominantly single excited states, the D-ΔMBPT(2) method is not expected to perform well. Even though the D-ΔMBPT(2) is presented as a direct method to compute IPs, EAs, and excitation energies, the wave function of the excited state can be obtained as a perturbative expansion of the relaxed Hartree-Fock excited state. A disadvantage, in common with the ΔHF method, is that the excited-state wave function is not orthogonal to the ground-state wave function, whereas the exact wave function is.

We applied the ΔMBPT(2) and D-ΔMBPT(2) methods to calculate IPs and excitation energies of small molecules. The ΔMBPT(2) values are the optimal values that can be obtained with the numerical integration procedure (D-ΔMBPT(2) method) and are very promising. For IPs, the performance is slightly better than that of an iterative second-order solution to the Dyson equation (TOEP2) using a transition operator method. For excitation energies, the comparison to EOM-CCSD values shows deviations below 0.5 eV. However, the use of the energy derivative in the numerical integration scheme reveals several difficulties, which will be subject of further research. First, residual relaxation effects beyond the Hartree-Fock level are important. If the MBPT(2) energy instead of the Hartree-Fock energy is made stationary with respect to orbital change, the integration of the energy derivative yields the ΔMBPT(2) values. Second, when the orbital has fractional occupation, the orbital resumes the role of an occupied and an unoccupied orbital in the correlated expression. This can cause the denominator to become small and the second-order energy derivative to behave erratically, particularly when higher-order terms are included, where the

denominator is quadratic in the orbital energy difference. Third, the Hartree-Fock solution has to be converged carefully to avoid sudden changes in the electronic solution as the occupation number varies.

ACKNOWLEDGMENTS

This work was sponsored by the Office of Basic Energy Sciences and by the Office of Advanced Scientific Computing Research, U.S. Department of Energy under Contract No. DE-AC05-00OR22725. It was also supported by an allocation of advanced computing resources provided by the National Science Foundation; some computations were performed on Kraken at the National Institute for Computational Sciences. One of the authors (J.V.O.) acknowledges support from the National Science Foundation to Auburn University through Grant No. CHE-0809199.

APPENDIX: PARTIAL DERIVATIVES FOR EXCITATION ENERGIES

The partial derivative of the second-order energy with respect to n_r with fractional occupation of orbital r and s is given by

$$
\begin{aligned}
\left.\frac{\partial E_c^{(2)}}{\partial n_r}\right|_{0<n_s<1} = {} & \frac{1}{2}\sum_{j\neq s}^{occ}\sum_{bc\neq rs}^{virt}\frac{\langle jr\|bc\rangle^2}{\epsilon_j+\epsilon_r-\epsilon_b-\epsilon_c}+\frac{1}{2}\sum_{bc\neq rs}^{virt} n_s\frac{\langle sr\|bc\rangle^2}{\epsilon_s+\epsilon_r-\epsilon_b-\epsilon_c}\\
& +2\sum_{b\neq s}^{virt} n_s(1-n_r)\frac{\langle sr\|br\rangle^2}{\epsilon_s-\epsilon_b}+2\sum_{b\neq r}^{virt} n_s(1-n_s)\frac{\langle sr\|bs\rangle^2}{\epsilon_r-\epsilon_b}\\
& +\sum_{j\neq s}^{occ}\sum_{b\neq s}^{virt}(1-n_r)\frac{\langle jr\|br\rangle^2}{\epsilon_j-\epsilon_b}+2\sum_{j\neq s}^{occ}(1-n_r)(1-n_s)\frac{\langle jr\|sr\rangle^2}{\epsilon_j-\epsilon_s}\\
& +\sum_{j\neq s}^{occ}\sum_{b\neq r}^{virt}(1-n_s)\frac{\langle jr\|bs\rangle^2}{\epsilon_j+\epsilon_r-\epsilon_b-\epsilon_s} \qquad (I)/(IV)\\
& -\frac{1}{2}\sum_{jk\neq rs}^{occ}\sum_{b\neq s}^{virt}\frac{\langle jk\|rb\rangle^2}{\epsilon_j+\epsilon_k-\epsilon_r-\epsilon_b}-\sum_{j\neq s}^{occ}\sum_{b\neq s}^{virt} n_r\frac{\langle jr\|rb\rangle^2}{\epsilon_j-\epsilon_b}\\
& -2\sum_{b\neq s}^{virt} n_r n_s\frac{\langle sr\|rb\rangle^2}{\epsilon_s-\epsilon_b}-2\sum_{j\neq s}^{occ} n_r(1-n_s)\frac{\langle jr\|rs\rangle^2}{\epsilon_j-\epsilon_s}\\
& -\sum_{j\neq r}^{occ}\sum_{b\neq s}^{virt} n_s\frac{\langle js\|rb\rangle^2}{\epsilon_j+\epsilon_s-\epsilon_r-\epsilon_b}-2\sum_{j\neq r}^{occ} n_s(1-n_s)\frac{\langle js\|rs\rangle^2}{\epsilon_j-\epsilon_r}\\
& -\frac{1}{2}\sum_{jk\neq rs}^{occ}(1-n_s)\frac{\langle jk\|rs\rangle^2}{\epsilon_j+\epsilon_k-\epsilon_r-\epsilon_s} \qquad (II)/(V)\\
& +\text{higher}-\text{order terms}.
\end{aligned}
$$

The higher-order terms are written as

$$
\begin{aligned}
HOT|_{0<n_s<1} = {} & -\frac{1}{4}\sum_{jk\neq rs}^{occ}\sum_{bc\neq rs}^{virt}\frac{\langle kj\|bc\rangle^2}{(\epsilon_k+\epsilon_j-\epsilon_b-\epsilon_c)^2}\times(\langle rk\|rk\rangle+\langle rj\|rj\rangle-\langle rb\|rb\rangle-\langle rc\|rc\rangle)\\
& -\frac{1}{2}\sum_{j\neq s}^{occ}\sum_{bc\neq rs}^{virt} n_r\frac{\langle rj\|bc\rangle^2}{(\epsilon_r+\epsilon_j-\epsilon_b-\epsilon_c)^2}\times(\langle rj\|rj\rangle-\langle rb\|rb\rangle-\langle rc\|rc\rangle)\\
& -\sum_{bc\neq rs}^{virt} n_r n_s\frac{\langle rs\|bc\rangle^2}{(\epsilon_r+\epsilon_s-\epsilon_b-\epsilon_c)^2}\times(\langle rs\|rs\rangle-\langle rb\|rb\rangle-\langle rc\|rc\rangle)\\
& -6\sum_{b\neq s}^{virt} n_r n_s(1-n_r)\frac{\langle rs\|br\rangle^2}{(\epsilon_s-\epsilon_b)^2}\times(\langle rs\|rs\rangle-\langle rb\|rb\rangle)
\end{aligned}
$$

$$+6\sum_{b\neq r}^{virt} n_r n_s(1-n_s)\frac{\langle rs\|bs\rangle^2}{(\epsilon_r-\epsilon_b)^2}\times\langle rb\|rb\rangle$$

$$-2\sum_{j\neq s}^{occ}\sum_{b\neq s}^{virt} n_r(1-n_r)\frac{\langle rj\|br\rangle^2}{(\epsilon_j-\epsilon_b)^2}\times(\langle rj\|rj\rangle-\langle rb\|rb\rangle)$$

$$-6\sum_{j\neq s}^{occ} n_r(1-n_r)(1-n_s)\frac{\langle rj\|sr\rangle^2}{(\epsilon_j-\epsilon_s)^2}\times(\langle rj\|rj\rangle-\langle rs\|rs\rangle)$$

$$-2\sum_{j\neq s}^{occ}\sum_{b\neq r}^{virt} n_r(1-n_s)\frac{\langle rj\|bs\rangle^2}{(\epsilon_r+\epsilon_j-\epsilon_b-\epsilon_s)^2}\times(\langle rj\|rj\rangle-\langle rb\|rb\rangle-\langle rs\|rs\rangle)$$

$$-\frac{1}{2}\sum_{j\neq r}^{occ}\sum_{bc\neq rs}^{virt} n_s\frac{\langle sj\|bc\rangle^2}{(\epsilon_s+\epsilon_j-\epsilon_b-\epsilon_c)^2}\times(\langle rs\|rs\rangle+\langle rj\|rj\rangle-\langle rb\|rb\rangle-\langle rc\|rc\rangle)$$

$$-2\sum_{j\neq r}^{occ}\sum_{b\neq s}^{virt} n_s(1-n_r)\frac{\langle sj\|br\rangle^2}{(\epsilon_s+\epsilon_j-\epsilon_b-\epsilon_r)^2}\times(\langle rs\|rs\rangle+\langle rj\|rj\rangle-\langle rb\|rb\rangle)$$

$$-6\sum_{j\neq r}^{occ} n_s(1-n_r)(1-n_s)\frac{\langle sj\|sr\rangle^2}{(\epsilon_j-\epsilon_r)^2}\times\langle rj\|rj\rangle$$

$$-2\sum_{j\neq r}^{occ}\sum_{b\neq r}^{virt} n_s(1-n_s)\frac{\langle sj\|bs\rangle^2}{(\epsilon_j-\epsilon_b)^2}\times(\langle rj\|rj\rangle-\langle rb\|rb\rangle)$$

$$-\frac{1}{2}\sum_{jk\neq rs}^{occ}\sum_{b\neq s}^{virt}(1-n_r)\frac{\langle kj\|br\rangle^2}{(\epsilon_k+\epsilon_j-\epsilon_b-\epsilon_r)^2}\times(\langle rk\|rk\rangle+\langle rj\|rj\rangle-\langle rb\|rb\rangle)$$

$$-\sum_{jk\neq rs}^{occ}(1-n_r)(1-n_s)\frac{\langle kj\|sr\rangle^2}{(\epsilon_k+\epsilon_j-\epsilon_s-\epsilon_r)^2}\times(\langle rk\|rk\rangle+\langle rj\|rj\rangle-\langle rs\|rs\rangle)$$

$$-\frac{1}{2}\sum_{jk\neq rs}^{occ}\sum_{b\neq r}^{virt}(1-n_s)\frac{\langle kj\|bs\rangle^2}{(\epsilon_k+\epsilon_j-\epsilon_b-\epsilon_s)^2}\times(\langle rk\|rk\rangle+\langle rj\|rj\rangle-\langle rb\|rb\rangle-\langle rs\|rs\rangle)$$

$$(III)/(VI).$$

[1] A. Szabo and N. S. Ostlund, *Modern Quantum Chemistry: Introduction to Advanced Electronic Structure Theory* (Dover, 1996).
[2] J. F. Stanton and R. J. Bartlett, J. Chem. Phys. **98**, 7029 (1993).
[3] R. J. Bartlett, *in Modern Electronic Structure Theory* (World Scientific, Singapore, 1995).
[4] I. Lindgren, Int. J. Quantum Chem. **14**(S12), 33 (1978).
[5] M. A. Haque and D. Mukherjee, J. Chem. Phys. **80**, 5058 (1984).
[6] J. V. Ortiz, "The electron propagator picture of molecular electronic structure," in *Computational Chemistry: Reviews of Current Trends* (World Scientific, Singapore, 1997), pp. 1–61.
[7] A. Stan, N. E. Dahlen, and R. van Leeuwen, J. Chem. Phys. **130**, 114105 (2009).
[8] J. Linderberg and Y. Öhrn, *Propagators in Quantum Chemistry*, 2nd ed. (Wiley, 2004).
[9] P. Jørgensen, Annu. Rev. Phys. Chem. **26**, 359 (1975).
[10] E. K. Gross, J. F. Dobson, and M. Petersilka, *Topics in Current Chemistry: Density Functional Theory of Time-Dependent Phenomena*, Density Functional Theory II Vol. 181 (Springer-Verlag, Berlin/Heidelberg, 1996).
[11] J. B. Foresman, M. Head-Gordon, and J. A. Pople, J. Phys. Chem. **96**, 135 (1992).
[12] A. Beste, R. J. Harrison, and T. Janai, J. Chem. Phys. **125**, 074101 (2006).
[13] J. G. Kirkwood, J. Chem. Phys. **3**, 300 (1935).
[14] R. W. Zwanzig, J. Chem. Phys. **22**, 1420 (1954).
[15] R. G. Parr and W. Yang, *Density-Functional Theory of Atoms and Molecules* (Oxford University Press, New York, 1989).
[16] H. J. Kim and R. G. Parr, J. Chem. Phys. **41**, 2892 (1964).
[17] M. Musial, A. Perera, and R. J. Bartlett, J. Chem. Phys. **134**, 114108 (2011).
[18] J. C. Slater, *Quantum Theory of Molecules and Solids* (McGraw-Hill, New York, 1974).
[19] A. R. Williams, R. A. deGroot, and C. B. Sommers, J. Chem. Phys. **63**, 628 (1975).
[20] M. E. McHenry, R. C. O'Handley, and K. H. Johnson, Phys. Rev. B **35**, 3555 (1987).
[21] P. Verma and R. J. Bartlett, J. Chem. Phys. **137**, 134102 (2012).
[22] O. Goscinski, G. Howat, and T. Åberg, J. Phys. B **8**, 11 (1975).
[23] O. Goscinski, B. T. Pickup, and G. Purvis, Chem. Phys. Lett. **22**, 167 (1973).
[24] R. Flores-Moreno, V. G. Zakrzewski, and J. V. Ortiz, J. Chem. Phys. **127**, 134106 (2007).
[25] J.-P. Blaizot and G. Ripka, *Quantum Theory of Finite Systems* (MIT, Cambridge/Massachusetts, 1986).
[26] K. J. H. Giesbertz and E. J. Baerends, J. Chem. Phys. **132**, 194108 (2010).
[27] I. Shavitt and R. J. Bartlett, *Many-Body Methods in Chemistry and Physics, MBPT and Coupled-Cluster Theory* (Cambridge University Press, New York, 2009).

[28]A. J. Cohen, P. Mori-Sánchez, and W. Yang, J. Chem. Theory Comput. **5**, 786 (2009).
[29]J. P. Perdew, R. G. Parr, M. Levy, and J. L. Balduz, Jr., Phys. Rev. Lett. **49**, 1691 (1982).
[30]A. Beste and R. J. Bartlett, J. Chem. Phys. **120**, 8395 (2004).
[31]A. Beste and R. J. Bartlett, J. Chem. Phys. **123**, 154103 (2005).
[32]G. D. Purvis and Y. Öhrn, Chem. Phys. Lett. **33**, 396 (1975).
[33]J. Simons and W. D. Smith, J. Chem. Phys. **58**, 4899 (1973).
[34]L. S. Cederbaum, Theor. Chim. Acta. **31**, 239 (1973).
[35]B. T. Pickup and O. Goscinski, Mol. Phys. **26**, 1013 (1973).
[36]M. Head-Gordon, R. J. Rico, M. Oumi, and T. J. Lee, Chem. Phys. Lett. **219**, 21 (1994).
[37]For an in depth discussion of size intensivity versus size extensivity see T. Shiozaki, K. Hirao, and S. Hirata, J. Chem. Phys. **126**, 244106 (2007).
[38]S. Grimme and E. I. Izgorodina, Chem. Phys. **305**, 223 (2004).
[39]Y. M. Rhee and M. Head-Gordon, J. Phys. Chem. A **111**, 5314 (2007).
[40]A. Hellweg, S. A. Grün, and C. Hättig, Phys. Chem. Chem. Phys. **10**, 4119 (2008).
[41]N. O. C. Winter and C. Hättig, J. Chem. Phys. **134**, 184101 (2011).
[42]M. Feyereisen, G. Fitzgerald, and A. Komornicki, Chem. Phys. Lett. **208**, 359 (1993).
[43]J. Deng and P. M. W. Gill, J. Chem. Phys. **134**, 081103 (2011).
[44]M. Valiev, E. Bylaska, N. Govind, K. Kowalski, T. Straatsma, H. van Dam, D. Wang, J. Nieplocha, E. Apra, T. Windus *et al.*, Comput. Phys. Commun. **181**, 1477 (2010).
[45]T. H. Dunning and P. J. Harrison, *in Modern Theoretical Chemistry* (Plenum, New York, 1977).
[46]See supplementary material at http://dx.doi.org/10.1063/1.4790626 for basis set dependence, Legendre-Gauss quadrature convergence, and energies and energy derivatives as a function of occupation for H_2O, and selected energies and energy derivatives as a function of occupation for CH_2O and NH_3.
[47]M. W. Schmidt, K. K. Baldridge, J. A. Boatz, S. T. Elbert, M. S. Gordon, J. H. Jensen, S. Koseki, N. Matsunaga, K. A. Nguyen, S. Su, *et al.*, J. Comput. Chem. **14**, 1347 (1993).
[48]J. Garza, J. A. Nichols, and D. A. Dixon, J. Chem. Phys. **113**, 6029 (2000).
[49]T. J. Watson and R. J. Bartlett, Chem. Phys. Lett. **555**, 235 (2013).
[50]W. L. Jolly, K. D. Bomben, and C. J. Eyermann, At. Data Nucl. Data Tables **31**, 433 (1984).
[51]K. Kimura, S. Katsumata, Y. Achiba, T. Yamazaki, and S. Iwata, *Handbook of HeI Photoelectron Spectra of Fundamental Organic Molecules. Ionization Energies, Ab Initio Assignments, and Valence Electronic Structure for 200 Molecules* (Halsted, New York, 1981).
[52]R. J. Rico, T. J. Lee, and M. Head-Gordon, Chem. Phys. Lett. **218**, 139 (1994).
[53]G. Herzberg, *Molecular Spectra and Molecular Structure III. Electronic Spectra and Electronic Structure of Polyatomic Molecules* (Van Nostrand, Princeton, NJ, 1966).
[54]S. B. Ben-Shlomo and U. Kaldor, J. Chem. Phys. **92**, 3680 (1990).
[55]D. C. Comeau and R. J. Bartlett, Chem. Phys. Lett. **207**, 414 (1993).